International Journal of Fatigue 94 (2017) 97–109

Contents lists available at ScienceDirect

International Journal of Fatigue

journal homepage: www.elsevier.com/locate/ijfatigue

Mode-II total fatigue life model for unidirectional IM7/8552 carbon/epoxy composite laminate

Raghu Panduranga *, Kunigal Shivakumar

Center for Composite Materials Research, Department of Mechanical Engineering, North Carolina A&T State University, 1601 East Market Street, 205 Fort IRC Bldg, Greensboro, NC 27411, USA

ARTICLE INFO

Article history:
Received 16 December 2015
Received in revised form 20 May 2016
Accepted 19 September 2016
Available online 20 September 2016

Keywords:
Mode-II fatigue
Total fatigue life model
Delamination onset
Fatigue growth rate
IM7/8552
Fracture

ABSTRACT

This paper presents a method of developing Total Fatigue Life Model (TFLM) for a unidirectional composite laminate with a delamination subjected to mode-II stress state. The model includes three domains of delamination growth rates: the middle Paris domain and the two end, onset and fracture, domains. The constants in the equation were determined from fracture and fatigue test data of End Notched Flexure (ENF) specimens for IM7/8552 carbon/epoxy composite laminate. The mode-II fracture toughness, G_{IIc} was determined from fracture test and it was found to be 0.978 kJ/m^2. The fatigue crack growth rate data was generated for different initial G_{IIimax} values by load controlled constant amplitude cyclic load fatigue tests for a stress ratio (R) of 0.1. The fatigue threshold energy release rate, G_{IIth} based on 1% compliance change for one million cycles (N) was found to be $0.167G_{IIc}$. The generated fatigue test results da/dN versus G_{IImax}/G_{IIc} was found to follow the equation $0.8(G_{IImax}/G_{IIc})^{5.8}$ $((1-(G_{IIth}/G_{IImax})^{12})/(1-(G_{IImax}/G_{IIc})^{3}))$ for IM7/8552 carbon/epoxy composite laminate. The Paris law exponent (β) agreed well with the values reported in the literature. The test data also demonstrated that a single fatigue test at $G_{IIimax} = 0.3G_{IIc}$, would be sufficient to generate the complete da/dN growth rate data instead of multiple specimen tests at different values of G_{IIimax}.

1. Introduction

Delamination is a primary failure mode in polymer matrix composite laminates [1–4]. Delamination is typically characterized based on linear elastic fracture mechanics (LEFM) using the energy release rate, G, which quantifies material's resistance to delamination. The Knowledge of material's resistance to interlaminar fracture and fatigue is essential to establish design allowable and damage tolerance guidelines for composite structures. Delamination growth rate models are essential in damage tolerant design of structures in order to predict fatigue life and establish appropriate inspection intervals so that a delamination can be found and repaired long before the delamination reaches critical size. Fatigue delamination growth laws that cover the threshold/onset, the stable growth and the unstable fracture domains (see Fig. 1) are needed for total life estimation. Such crack growth laws were proposed for metallic materials [5] and are becoming accepted in damage tolerant design of fixed-wing aircrafts. Similar total life methodology that includes damage onset, growth and fracture is needed for composite laminates. A first attempt was made by Shivakumar et al. [6–8] to develop a Total Fatigue Life Model (TFLM) for mode-I loaded E-glass/vinyl ester woven roving composite laminate. Modification of Shivakumar et al.'s equation were experimented in [9] for typical and aggressive block loaded test samples and concluded that the original G_{IR}-normalized growth model as suggested by Poursartip [10] is a better way of expressing total fatigue life equation. The same model was extended and applied to T800H/3900-2 carbon/epoxy composite laminate [11]. Chen et al. [12] applied the mode-I TFLM to T700 carbon/vinyl ester composite laminate and shown that TFL equation fits the test data very well in both subcritical and linear domains while giving the limited solution in unstable/fracture domain. Similar models are needed for mode-II and mixed-mode (I–II) loaded problems. This research is focused on application of TFLM to mode-II loaded composite laminates.

Substantial research [10,13–17] has been done in composite laminates on energy release rate (G) driven delamination growth laws that is valid in domain 2. The data was found to follow a power law equation in G_{IImax} or ΔG_{IImax} by curve fits. Research efforts were made also on the effect of stress ratio [13,14], matrix toughness [15,16], pure and mixed-mode stress states [14,16,17], and cyclic compression [18]. Considerable research efforts were made also on the effect of interleaf types such as fine thermoplastic

* Corresponding author.
E-mail address: raghupanduranga@gmail.com (R. Panduranga).

http://dx.doi.org/10.1016/j.ijfatigue.2016.09.014
0142-1123/

Nomenclature

A	coefficient of compliance calibration equation
a	crack/delamination length
a_0	initial crack/delamination length
B	specimen width
C	compliance
C_0	initial compliance (at a_0)
CC	compliance calibration
D	coefficient of onset life equation
D_1	material constant in TFLM
D_2	material constant in TFLM
ENF	end notch flexure
FEP	fluorinated ethylene propylene
G_T	total energy release rate
G_{Imax}	Mode-I maximum energy release rate
G_{IR}	Mode-I fracture resistance
G_{IIc}	Mode-II fracture toughness (1/2 mil thick insert delamination)
G_{IImax}	Mode-II maximum energy release rate
G_{IIimax}	Mode-II initial maximum energy release rate
G_{IImin}	Mode-II minimum energy release rate
G_{II_NPC}	Mode-II NPC fracture toughness (1/2 mil thick insert delamination)
G_{II_PC}	Mode-II PC fracture toughness (shear precracked)
G_{IIth}	Mode-II threshold energy release rate
h	specimen half-thickness
m	coefficient of compliance calibration equation
MA	moving average
n	exponent of onset life equation
N	number of cycles
$N_{1\%}$	Number of cycles required for 1% compliance change
NPC	no pre-crack (manufactured crack)
PC	shear pre-crack
P	load
P_c	fracture load
P_{max}	maximum load
P_{min}	minimum load
R	cyclic load ratio
STD	standard deviation
TFLM	total fatigue life model
wMA	weighted moving average
α	coefficient of paris law
β	exponent of paris law
δ	displacement
$\Delta\delta$	peak-to-peak displacement
ΔN	difference between the cycle counts
ΔG_{II}	range of energy release rate
ΔP	peak-to-peak load

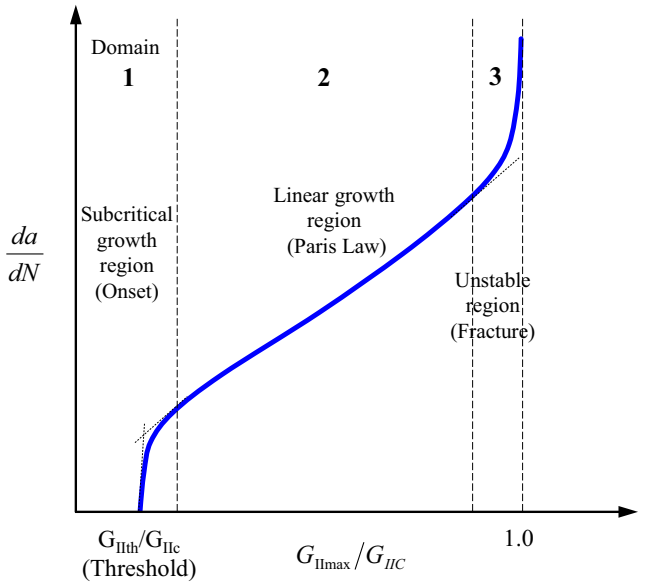

Fig. 1. Conceptual plot of da/dN versus G_{IImax}/G_{IIc}.

polyamide particles [19], self-same epoxy [20], Zanchor reinforcement (novel through-thickness reinforcement technique in which in-plane yarns are entangled with each other using special needles) [21], and Nylon 6,6 nanofibers [22] on the fatigue crack growth behavior of carbon/epoxy laminates under both mode-I and mode-II stress states. These studies show that interleaved composite laminates have significantly improved delamination fatigue threshold onset value and growth resistance when compared to base laminates.

O'Brien et al. [23] established mode-II fatigue growth rate equation for IM7/8552 carbon/epoxy laminates fabricated from prepregs supplied by two different sources but they focused on the Paris law domain (domain 2). Arguelles et al. [24] measured fatigue crack growth rates for AS4/3501-6 and AS4/8552 carbon/epoxy composites laminates under both mode-I and mode-II stress states and concluded that the delamination growth rate is higher for the brittle matrix (3501-6) laminates than the tough matrix (8552) laminates. This phenomenon was more apparent in mode-II loaded specimen. Recently, Murri [25] performed mode-I fatigue tests on IM7/8552 carbon/epoxy laminates at three loading levels (G_{Imax} equal to $0.5G_{Ic}$, $0.4G_{Ic}$, and $0.3G_{Ic}$) and developed Paris law type equation for delamination growth including the effects of fiber bridging (normalized by G_{IR}). Ratcliffe and Johnston Jr. [26] conducted fracture tests on IM7/8552 tape laminates at three mixed-mode ratios $G_{II}/G_T = 0.2$, 0.5, and 0.8 and delamination fatigue tests at each mixed-mode ratio for G_{max} values of $0.5G_c$, $0.4G_c$, $0.3G_c$, and $0.2G_c$. They developed fatigue growth rate equation for domain 2 and found that the delamination growth rate increased monotonically with G_{II}/G_T ratio. The data reduction procedure used in [23,25,26] was both parsing and incremental polynomial method as given in ASTM E647 [27].

As mentioned above, numerous researchers have carried out fatigue delamination characterization on composite laminates. But there was a limited effort on developing a Total Fatigue Life Model (TFLM) for composite laminates and there is no literature on TFLM for mode-II and mixed-mode stress states. The objective of this paper is to develop a mode-II Total Fatigue Life Model for IM7/8552 carbon/epoxy laminates similar to that of mode-I TFLM developed previously for Glass/Vinyl Ester Composites [6–9]. In this paper, the mode-II interlaminar fracture toughness, G_{IIc}, is measured from ENF test specimen. Mode-II fatigue tests are conducted at stress ratio (R) of 0.1 for initial G_{IIimax} values ranging from 0.2 to $0.6G_{IIc}$. The parsing technique and weighted moving average data smoothing methods is used to reduce fatigue growth data. Fatigue threshold energy release rate (G_{IIth}) and fatigue growth rate are determined from fatigue test results. Finally, an empirical mode-II total fatigue life equation was established for unidirectional IM7/8552 carbon/epoxy composite laminate.

2. Modeling approach/methodology

The methodology and test procedures for developing total fatigue life model are briefly explained below.

2.1. Assumptions

1. The da/dN is proportional to the driving force G_{IImax}.
2. The da/dN is bounded by two extreme values of G_{IImax}; the threshold energy release rate G_{IIth} (at or below which da/dN is nearly zero or no delamination growth) and the G_{IIc}, at which da/dN is very large or specimen fractures.
3. The value of G_{IIth} can be determined by 1% change in compliance of the fatigue test specimen.
4. The da/dN data is measured from load-controlled fatigue test until the specimen fractures.

2.2. Approach

This approach is similar to the one described in references [6–9]. The da/dN data for composite laminates falls into three domains, namely, subcritical or slow delamination growth domain, G_{IImax} controlled domain (or Paris' domain), and the unstable or fracture domain (see Fig. 1). From the assumption 1, the da/dN in domain 2 is written in a power law form as

$$\frac{da}{dN} = \alpha\left(\frac{G_{IImax}}{G_{IIc}}\right)^{\beta} \tag{1}$$

where α and β are material constants determined from the curve fit to the test data.

In the subcritical domain, the da/dN (assumption 2) varies between zero (when $G_{IImax} \leqslant G_{IIth}$) and a value that matches domain 2. The form of the da/dN equation in this domain can be written as

$$\frac{da}{dN} = \alpha\left(\frac{G_{IImax}}{G_{IIc}}\right)^{\beta}\left[1-\left(\frac{G_{IIth}}{G_{IImax}}\right)^{D_1}\right] \quad \text{for} \quad G_{IImax} \geq G_{IIth} \tag{2}$$

The exponent D_1 is determined from curve fit to the test data.

In the unstable domain, da/dN varies between ∞ (when $G_{IImax} = G_{IIc}$) and the transition value that matches Eq. (1) in domain 2. The form of the da/dN equation in this domain can be written as

$$\frac{da}{dN} = \alpha\left(\frac{G_{IImax}}{G_{IIc}}\right)^{\beta}\frac{1}{\left[1-\left(\frac{G_{IImax}}{G_{IIc}}\right)^{D_2}\right]} \quad \text{for } G_{IImax} \leq G_{IIc} \tag{3}$$

The exponent D_2 is a material parameter determined from the curve fit to the test data.

Finally, the combined da/dN equation that covers all three domains is

$$\frac{da}{dN} = \alpha\left(\frac{G_{IImax}}{G_{IIc}}\right)^{\beta}\frac{\left[1-\left(\frac{G_{IIth}}{G_{IImax}}\right)^{D_1}\right]}{\left[1-\left(\frac{G_{IImax}}{G_{IIc}}\right)^{D_2}\right]} \quad \text{valid for } G_{IIth} \leq G_{IImax} \leq G_{IIc} \tag{4}$$

The values of α, β, D_1 and D_2 are the material parameters determined by curve fit to the fatigue test data.

2.3. Test procedure for establishing the parameters

(a) Conduct mode-II fracture test using the End Notch Flexure (ENF) specimen as per ASTM D7905M-14 [28] and determine G_{IIc}.

(b) Conduct the compliance calibration (CC) tests at a_0 = 15.24, 25.4, and 35.56 mm as per the ASTM D7905M-14. Establish relation between compliance (C) and crack length (a) by plotting compliance against the corresponding crack lengths raised to the third power and fit a line given by Eq. (5).

$$C = A + ma^3 \tag{5}$$

Determine CC coefficients, m and A, using a least-squares linear regression analysis of the compliance, C, versus crack length cubed (a^3) where A is the intercept and m is the slope obtained from the regression analysis.

(c) Conduct a constant amplitude load controlled fatigue growth test at four loading levels, G_{IImax} equal to about $0.6G_{IIc}$, $0.5G_{IIc}$, $0.4G_{IIc}$, and $0.3G_{IIc}$ at loading frequency of 1 Hz and R = 0.1. Establish the G_{IIth} by a power law curve fit to G_{IImax} versus $N_{1\%}$ (onset life) data, where $N_{1\%}$ is the number of cycles required to change the initial compliance by 1%. Also note that 1% compliance change is an arbitrary criterion established by ASTM for unidirectional prepreg composites. This value can be changed to an acceptable value. For example, textile composites need 2% or 5% compliance change criteria to establish G_{IIth}.

(d) Repeat the test at least for two specimens and plot the data as da/dN versus G_{IImax} on a log-log graph.

(e) Divide the plot into three domains by visual inspection (see Fig. 1). The middle linear domain and the two ends, namely subcritical and unstable domains.

(f) Perform least square log-log fit to the domain 2 data and determine the constants α and β. The domain 2 is part of the fatigue growth rate data from $1.3G_{IImax}$ to $0.7G_{IIc}$.

(g) Determine D_1 in Eq. (2), using already determined α and β by fitting the equation to domains 1 and 2 data by a trial and error approach. A suggestion is to use the data from G_{IIth} to $1.3G_{IImax}$.

(h) Finally determine D_2 in Eq. (3) by fitting the equation to domains 2 and 3 data as in step 'g'. A suggestion is to use the data from $0.7G_{IIc}$ to G_{IIc} (fracture).

(i) Using the constants determined above, plot Eq. (4) and compare it with the test data. If the fit is not satisfactory repeat steps 'e' through 'i'.

3. Materials and specimen fabrication

The material used in this study was IM7/8552 carbon/epoxy prepreg supplied by Hexcel Composites, USA. The panels were made of 24-ply unidirectional prepregs and a Fluorinated Ethylene Propylene (FEP) insert of 12.7 μm (0.5 mil) thick was placed between the 12th and 13th plies to create an initial delamination. The panels were made in an autoclave as per the guidance provided by the prepreg manufacturer. The stacking sequence of the laminate was $[0^0_{12}/\text{Insert}/0^0_{12}]$. For all fatigue specimens, the panel was cut to 152 mm length (6 in.) × 25.4 mm width (1 in.) specimens in such a way that the end of the FEP insert is about 50.8 mm (2 in.) from the end of the panel. The dimension of the fracture specimens was 177.8 mm length (7 in.) × 25.4 mm width (1 in.) with an insert length of 76.2 mm (3 in.). All the panels were cut using a tile saw having a diamond coated blade. Specimens were dried overnight at 60 °C prior to testing. After drying, the width and thickness of each specimen were measured to the nearest 0.001 mm, using a micrometer, at the center and at each end. The measured fatigue specimen dimensions are listed in Table 1. The average specimen width, b, was 25.52 mm (1.005 in.) and the average specimen thickness, 2 h, was 3.84 mm (0.151 in.). Fig. 2 shows the ENF specimen configuration used for fracture and fatigue tests. The initial delamination

Table 1
Fatigue test specimen dimensions and compliance parameters.

Specimen #	G_{IIimax}/G_{IIc}	G_{IIimax}, kJ/m^2	Width B, mm	Thickness 2h, mm	a_0, mm	a, mm	a^3, mm^3	C, mm/N	A	m
I8E1–1	0.6	0.59	25.48	3.78	25.4	15.2	3540	1.614E–03	1.559E–03	1.835E–08
			25.48	3.81		25.4	16,387	1.873E–03		
			25.50	3.78		35.6	44,966	2.380E–03		
I8E1–2	0.5	0.49	25.55	3.78	25.4	15.2	3540	1.584E–03	1.525E–03	1.693E–08
			25.55	3.84		25.4	16,387	1.806E–03		
			25.55	3.81		35.6	44,966	2.286E–03		
I8E1–3	0.4	0.39	25.53	3.78	25.4	15.2	3540	1.578E–03	1.519E–03	1.732E–08
			25.53	3.84		25.4	16,387	1.806E–03		
			25.53	3.81		35.6	44,966	2.297E–03		
I8E1–4	0.3	0.29	25.53	3.78	25.4	15.2	3540	1.601E–03	1.545E–03	1.739E–08
			25.53	3.81		25.4	16,387	1.836E–03		
			25.53	3.81		35.6	44,966	2.324E–03		
I8E1–5	0.2	0.20	25.48	3.79	25.4	15.2	3540	1.830E–03	1.755E–03	1.891E–08
			25.48	3.80		25.4	16,387	2.054E–03		
			25.48	3.81		35.6	44,966	2.609E–03		
I8E1–6	0.6	0.59	25.55	3.84	25.4	15.2	3540	1.530E–03	1.478E–03	1.645E–08
			25.55	3.89		25.4	16,387	1.756E–03		
			25.55	3.89		35.6	44,966	2.215E–03		
I8E1–7	0.5	0.49	25.53	3.86	25.4	15.2	3540	1.494E–03	1.439E–03	1.620E–08
			25.53	3.91		25.4	16,387	1.706E–03		
			25.53	3.91		35.6	44,966	2.167E–03		
I8E1–8	0.4	0.39	25.53	3.86	25.4	15.2	3540	1.495E–03	1.441E–03	1.602E–08
			25.53	3.91		25.4	16,387	1.707E–03		
			25.53	3.91		35.6	44,966	2.160E–03		
I8E1–9	0.3	0.29	25.53	3.86	25.4	15.2	3540	1.520E–03	1.467E–03	1.647E–08
			25.53	3.89		25.4	16,387	1.745E–03		
			25.53	3.91		35.6	44,966	2.205E–03		
I8E1–10	0.2	0.20	25.50	3.85	25.4	15.2	3540	1.593E–03	1.542E–03	1.703E–08
			25.48	3.88		25.4	16,387	1.834E–03		
			25.48	3.90		35.6	44,966	2.304E–03		

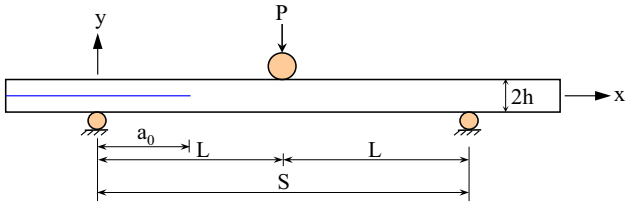

Fig. 2. End-notched flexure specimen configurations for fracture and fatigue tests.

length, a_0, is the distance from the left-support-point line (see Fig. 2) to the interior end of the insert, and was nominally 30.5 mm (1.2 in.) and 25.4 mm (1 in.) for fracture tests and fatigue tests, respectively. The density and fiber volume fraction of the laminate was measured in order to assess the quality of the fabricated laminate. The average density and fiber volume fraction of IM7/8552 laminate was 1.57 g/cc and 56%, respectively.

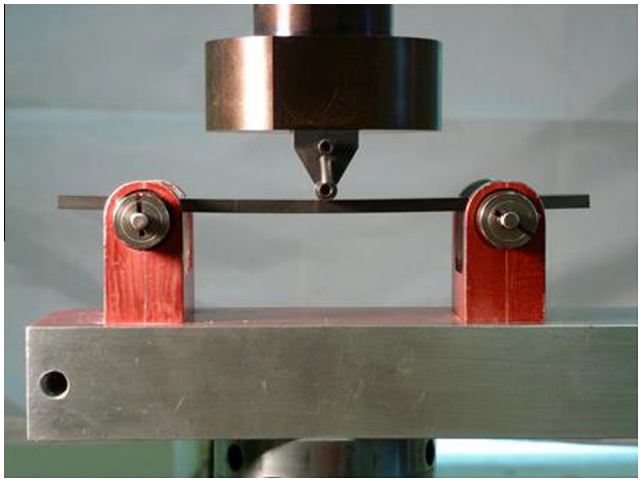

Fig. 3. Mode-II test set up.

4. Testing

All tests were carried out in an MTS 810 test machine using an End Notched Flexure (ENF) specimens. For fracture tests, a 1780 N (400 lb) load cell was used and for majority of fatigue tests an 890 N (200 lb) load cell was used. The test set up was the same for both fracture and fatigue tests and is shown in Fig. 3. Prior to fracture and fatigue tests, a compliance calibration was conducted for each specimen to determine the relationship between compliance and crack length. The compliance calibration relationship was used to estimate the crack length and to determine energy release rate, G_{II} levels during the fracture and fatigue tests. Fracture tests were conducted according to the ASTM D7905M-14 Test Standard [28]. The ASTM D7905M-14 test consisted of no pre-cracked (NPC) and pre-cracked (PC) fracture tests and determination of specimen compliance equation for both NPC and PC test specimens. The ASTM [28] uses compliance calibration approach for calculating G_{IIc}. The ASTM method uses the same specimen for measuring both manufactured crack (No precrack, NPC) G_{IIc_NPC} and shear precracked (PC) G_{IIc_PC} values. A thin polytetrafluoroethylene (PTFE, or Teflon) film of 12.7 μm (0.5 mil) thickness was inserted on the mid-plane to act as a crack starter for the NPC tests. The specimens were pre-cracked from this Teflon insert during the NPC fracture test to create a shear crack that mimic a naturally occurring crack. These shear precracked specimens were used in PC tests. There is no current ASTM standard for conducting

mode-II fatigue delamination characterization of unidirectional composite laminates. Fatigue tests were conducted in load control at five different maximum cyclic loads, P_{max}, corresponding to initial G_{IIimax} values of 60%, 50%, 40%, 30, and 20% of the average value of the G_{IIc_NPC}. Because the G_{IIimax} loading values are calculated based on G_{IIc_NPC}, the notations "G_{IIc}" and "G_{IIc_NPC}" are one and the same and is used interchangeably in the paper. The fatigue tests corresponding to $G_{IIimax}/G_{IIc} = 0.2$ loading were conducted only till the fatigue delamination onset life because the hydraulic fluid was leaking from the load frame's actuator beyond 119,194 load cycles. Therefore, the growth rate curves (da/dN vs. G_{IImax}) were not presented for $G_{IIimax}/G_{IIc} = 0.2$ loading. While conducting fatigue tests at $G_{IIimax}/G_{IIc} = 0.3$ and 0.2 loading, we observed that the specimen moves in x-direction whereas at $G_{IIimax}/G_{IIc} = 0.6$, 0.5, and 0.4 loading the specimen does not move. We used a drop of cyanoacrylate adhesive at the specimen support location in order to arrest the movement. After completing each PC fracture test and fatigue test, the specimen was split apart at the mid-plane so that the initial and final delamination lengths could be more accurately determined, and to verify that the delamination grew evenly across the specimen width. The details of the compliance calibration, fracture tests, and fatigue tests are described in the following sections.

4.1. Compliance calibration

Compliance calibration (CC) tests were performed for both fracture and fatigue test specimens. The details of the compliance measurement and determination of constants of the compliance equation are given in [28,29]. Compliance calibration tests for fracture and fatigue test specimens differ slightly. The compliance calibration for NPC and PC fracture test specimens involves measuring two compliance values at a = 20.32 and 40.64 mm in addition to compliance measurement at a = 30.48 mm (initial crack length for fracture test). In the case of fatigue test, the compliance was measured at a = 15.24, 25.40 and 35.56 mm, where the initial crack length for fatigue test was $a_0 = 25.4$ mm. For NPC and PC fracture specimens, CC tests were conducted at maximum loads of about 25% of critical load and whereas the CC tests for fatigue specimens were conducted at 178 N (40 lbs) so that the crack did not initiate or grow.

The CC tests were first performed on the NPC fracture specimens as follows. Three loadings were used to obtain three plots of load versus displacement. The three compliances are those from the two CC tests (at $a_0 - 10.16 = 20.32$ mm, and $a_0 + 10.16 = 40.64$ mm) and from the initial portion of the fracture test ($a_0 = 30.48$ mm). At each crack length, the compliance was determined from the least square fit to the linear portion of the displacement versus load (δ vs. P) data. The resulting compliances were plotted against the a^3 (see Fig. 4) and fitted a straight line as in Eq. (5). Fig. 4 shows a typical NPC fracture test fit of compliance as a function of crack length. The coefficients m and A for five NPC and five PC test specimens are listed in Table 2. The value of '*A*' varied between 1.47×10^{-3} and 1.58×10^{-3} and '*m*' varied between 1.61×10^{-8} and 1.78×10^{-8} for NPC tests while for PC tests '*A*' varied from 1.46×10^{-3} to 1.58×10^{-3} and '*m*' varied from 1.52×10^{-8} to 1.68×10^{-8}. The actual values of the NPC and PC specimen's *A* and *m* were used to calculate G_{IIc_NPC} and G_{IIc_PC}, respectively. Compliance calibration was repeated for each of the fatigue test specimens to determine CC coefficients *A* and *m*. The calculated *A* and *m* for all fatigue specimens are listed in Table 1.

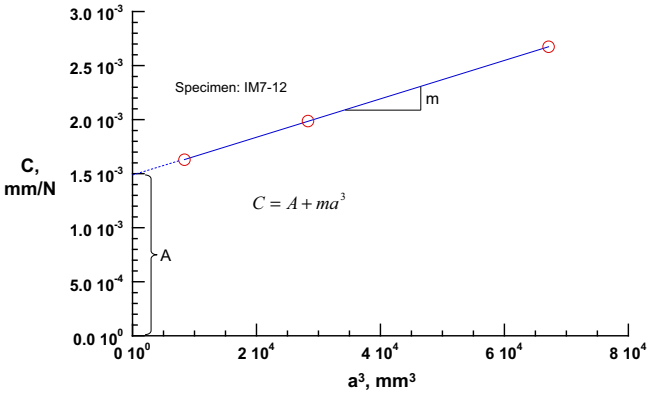

Fig. 4. Typical fit of C vs. a^3 for NPC fracture test.

4.2. Fracture test

The mode-II fracture test using the ENF specimen was conducted as per ASTM D7905M-14. Before each test, the specimen was viewed under an optical microscope to locate the end of the Teflon film which represents the initial crack tip location. This location was marked with a carbide-tipped scriber on the edge of the specimen while viewing under the microscope at 25× magnification. The procedure was repeated on the opposite edge. The mark was then seen under an illuminated magnifying glass while another scribe mark was made across the top of the specimen as the location of the crack front. The specimen was then placed in a 3-point bend fixture (Fig. 3) on a test machine with the span set at 101.6 mm (4 in.) as shown in Fig. 3. After establishing the compliance response of the test specimen, the fracture test was conducted for $a_0 = 30.48$ mm (1.2 in.) at a loading rate of 0.5 mm/min while recording the load and displacement at every 0.2 s until the first load drop (fracture load, P_c) was observed. The fracture

Table 2
ASTM 7905-14 fracture test results.

Test	Specimen #	Measured a, mm	B, mm	A	m	P_c, N	G_{IIc}, kJ/m^2
NPC	IM7-12	30.48	25.45	1.48E−03	1.78E−08	1015.3	1.003
	IM7-13	30.48	25.48	1.47E−03	1.73E−08	1070.3	1.081
	IM7-14	30.48	25.48	1.53E−03	1.70E−08	1032.3	0.990
	IM7-15	30.48	25.48	1.58E−03	1.66E−08	995.6	0.898
	IM7-16	30.48	25.48	1.52E−03	1.61E−08	1021.4	0.920
						Average (STD)	0.978 (0.073)
PC	IM7-12	30.48	25.45	1.48E−03	1.62E−08	899.3	0.716
	IM7-13	30.48	25.48	1.46E−03	1.57E−08	914.2	0.718
	IM7-14	30.48	25.48	1.53E−03	1.67E−08	863.8	0.683
	IM7-15	30.48	25.48	1.58E−03	1.68E−08	855.6	0.674
	IM7-16	30.48	25.48	1.51E−03	1.52E−08	911.0	0.689
						Average (STD)	0.696 (0.020)

load was recorded and the specimen was then unloaded at 0.5 mm/min to measure compliance and crack length after the test. Using the constant 'm' from the compliance equation, the G_{IIc} at fracture load P_c is calculated by;

$$G_{IIc} = 3m\frac{(P_c a)^2}{2B} \quad (6)$$

After completing the NPC fracture test, which created a shear pre-crack, the specimen was removed from the test machine and reused to conduct PC test with the crack length of 30.48 mm. The new delamination tip location was marked with the scriber on each edge of the specimen by viewing under an optical microscope and PC fracture tests were conducted using the new crack length of 30.48 mm with the same procedure as for the NPC test. Table 2 lists the specimen number, width, initial crack length (after corrections based on actual measurement after the test), CC coefficients, m and A, critical load (P_c), and calculated critical energy release rate for all specimens tested. The G_{IIc_NPC} varied from 0.898 to 1.081 kJ/m^2 with an average of 0.978 kJ/m^2, standard deviation of 0.073 kJ/m^2 or the coefficient of variation of about 7%. The G_{IIc_PC} varied from 0.674 to 0.718 kJ/m^2 with an average of 0.696 kJ/m^2, standard deviation of 0.02 kJ/m^2 or the coefficient of variation of about 3%. The difference between the NPC and PC fracture toughness is about 29%, a similar difference was reported in [23,29] for IM7/8552 composites. The difference between the NPC and PC test results reflect the well-known fact that the manufactured blunt crack requires more energy to pop open than the sharp crack in a PC specimen even though the resin film thickness is 12.7 μm (0.5 mil). The NPC fracture toughness (G_{IIc_NPC}) value is used as G_{IIc} of the material in all fatigue test data reduction and plots.

4.3. Fatigue test

The fatigue tests were conducted using manufactured/implanted delamination to measure delamination onset and growth using the same fixture as shown in Fig. 3. All fatigue and fracture test specimens were taken from the same panel fabricated by the autoclave process to avoid material and fabrication process variations. Specimens were subjected to sinusoidal cyclic loading at a frequency of 1 Hz and a cyclic loading ratio (P_{min}/P_{max}) of R = 0.1. Tests were conducted in load control at maximum cyclic loads, P_{max}, corresponding to G_{IIimax}/G_{IIc} ratios of 0.6, 0.5, 0.4, 0.3, and 0.2. Where G_{IIc} (0.978 kJ/m^2) is the average value of fracture toughness obtained from the NPC fracture tests. The maximum cyclic load level (P_{max}) was calculated from Eq. (6) for the specified G_{IIimax} value as follows.

$$P_{max} = \frac{1}{a_0}\left(\frac{2BG_{IIimax}}{3m}\right)^{1/2} \quad (7)$$

where a_0 is the initial delamination length for this fatigue test and B is the width of the specimen. Prior to fatigue testing, a compliance calibration was conducted as explained before to determine the CC coefficients *A* and *m* of the specimen (see Table 1). Table 3 lists the loading parameters, P_{max} and P_{min} values for all the fatigue specimens tested. An in-house developed LabView fatigue code was used for data accumulation and retrieval. During the fatigue testing, the computer system recorded peak-to-peak load (ΔP), peak-to-peak displacement (Δδ), compliance (C), and cycle count (N), at every cycle. This data was used to generate both delamination onset data and delamination growth rate. Specimens were cycled until there is sudden increase in compliance value (until the compliance is about 3 times the initial compliance value, C_0, which is an indication that the sample has fractured) or when the crack front reaches the load point. Then the fatigue test was stopped and the raw data file was saved to the hard disc for further data analysis. Note that in load control fatigue test, the P_{max} is constant but the delamination is growing continuously with number of cycles (N), consequently the applied G_{IImax} increases with N. After unloading, the specimens were pried open to measure the actual location of the initial crack front. Photos were taken of the two fracture surfaces of the specimen to obtain the fracture morphology.

Table 3
Loading parameters for fatigue testing.

Specimen #	G_{IIimax}/G_{IIc}	G_{IIimax}, kJ/m^2	Load, N	
			P_{max}	P_{min}
I8E1−1	0.6	0.59	917.9	91.8
I8E1−2	0.5	0.49	873.5	87.3
I8E1−3	0.4	0.39	772.0	77.2
I8E1−4	0.3	0.29	667.3	66.7
I8E1−5	0.2	0.20	522.0	52.2
I8E1−6	0.6	0.59	970.8	97.1
I8E1−7	0.5	0.49	892.4	89.2
I8E1−8	0.4	0.39	802.7	80.3
I8E1−9	0.3	0.29	685.7	68.6
I8E1−10	0.2	0.20	550.1	55.0

5. Data reduction

Fatigue test data reduction was conducted to determine delamination onset and growth rate curves for each specimen. The data acquisition system used during the fatigue tests provided a record of peak-to-peak (maximum-to-minimum) load (ΔP) and peak-to-peak displacement (Δδ) as a function of cycle count for the duration of the test for each cycle. From this data, the compliance was calculated by using the following expression.

$$C = \frac{\Delta\delta}{\Delta P} \quad (8)$$

From compliance C, the delamination length *a* was calculated from the *m* and *A* values of the specimen as follows.

$$a = \left(\frac{C - A}{m}\right)^{1/3} \quad (9)$$

Figs. 5–7 show a typical peak-to-peak load (ΔP), compliance (C), and the calculated delamination length (*a*) versus number of cycles (N), respectively for specimen I8E1−2. It is clear from Fig. 5 that in fatigue tests ΔP stabilization takes few cycles of loading and it was found to depend on fatigue cycling frequency. For 1 Hz loading frequency, it took about 6 cycles to stabilize the load, which is small

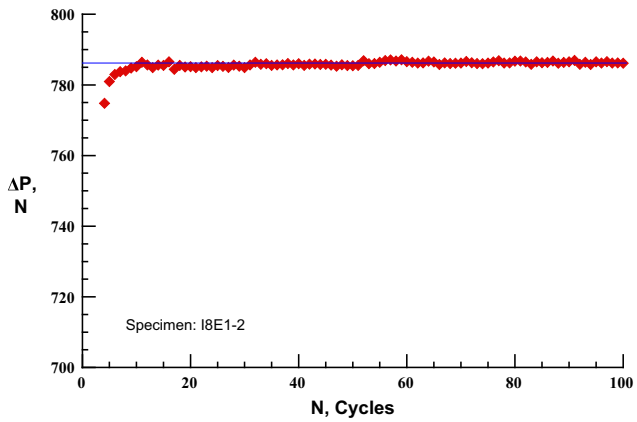

Fig. 5. Plot of load as a function of fatigue cycles.

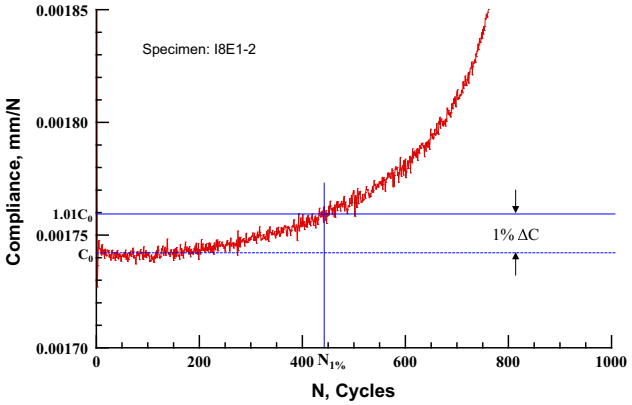

Fig. 6. Plot of compliance as a function of fatigue cycles and calculation of number of cycles for onset.

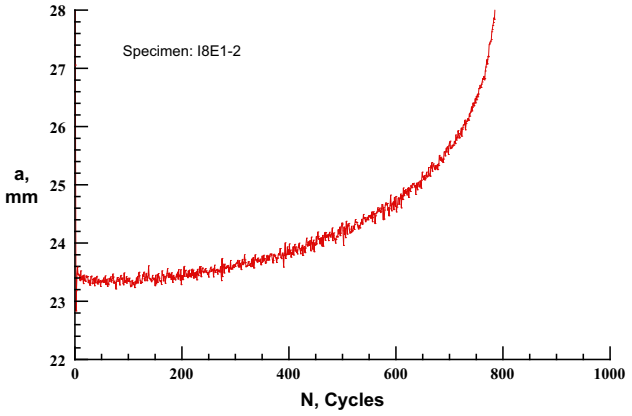

Fig. 7. Plot of crack length as a function of fatigue cycles.

compared to total number of cycles to damage onset or fracture. Therefore, this initial load stabilizing cycles is not considered in data analysis.

The three other parameters needed for the fatigue life prediction model are: number of cycles for onset, da/dN, and G_{IImax}. The ASTM standard D6115 [30] recommended two criteria to determine the number of cycles N for the onset of mode-I delamination growth, namely 1% and 5% increase of the compliance compared to initial compliance, C_0. In this work, the onset life $N_{1\%}$ for the applied G_{IIimax} is obtained from the 1% increase in compliance criterion. In Fig. 6, C_0 and $1.01C_0$ lines were drawn in order to determine $N_{1\%}$. The cycle corresponding to the point of intersection between $1.01C_0$ line and the C vs. N curve is the $N_{1\%}$. ASTM E647 [27] recommends two methods for determining the delamination growth rate, da/dN; a 2-point secant method and a 7-point incremental polynomial method. In the present work, only 2-point secant method was used for da/dN calculations of all test specimen data. Using the 2-point method, da/dN is determined from the slope of the line between two adjacent points on the plot of a vs. N as:

$$\left(\frac{da}{dN}\right)_i = \frac{a_{i+1} - a_i}{N_{i+1} - N_i} \tag{10}$$

where a_i is a crack length corresponding to cycle count N_i, and a_{i+1} and N_{i+1} are crack length and cycle count values corresponding to the next available data point. Then knowing the current a_i and P_{max}, the current $(G_{IImax})_i$ is calculated from Eq. (11).

$$(G_{IImax})_i = \frac{3m}{2B}(P_{max}a_i)^2 \tag{11}$$

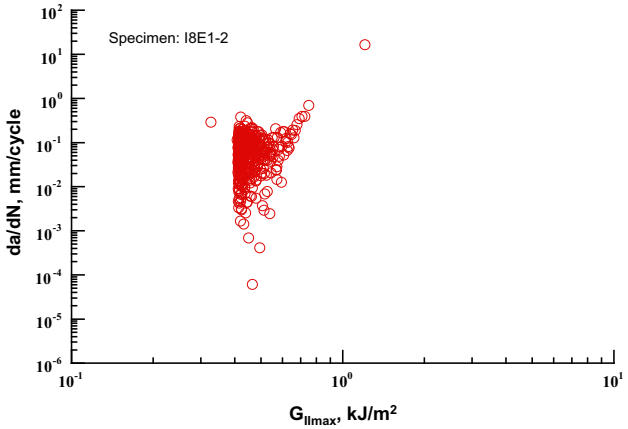

Fig. 8. Plot of delamination growth rate (da/dN) vs. G_{IImax}.

Finally, log-log plots of da/dN vs. G_{IImax} were generated. The plot of crack growth rate, da/dN versus G_{IImax} is shown in Fig. 8.

Note that because of cycle by cycle approach was used, a massive amount of data was generated during the fatigue test and also the fatigue data contained noise. Therefore, parsing and data smoothing using weighted Moving Average (wMA) method was used in this study. The data parsing and smoothing are described in the following sections.

5.1. Raw data parsing and smoothing

Because the fatigue raw data sets were very large and also noisy, a parsing routine was first applied to the raw data and then the data was smoothed using weighted moving average (wMA) method to eliminate noise and reduce the data set to a more manageable size. The noise in the raw data set can make it difficult to determine trends in the reduced G data. Parsing and smoothing removes most of the noise and therefore yields more useful reduced data. Raw fatigue data was parsed and smoothed using techniques such as parsing, graded parsing, moving average (MA), and weighted MA methods. All these methods were used individually and as well as in various combinations. After a lot of data smoothing experiments, it was found that graded parsing and weighted MA on compliance data followed by weighted MA on da/dN data resulted in more consistent and repeatable results.

The load cycle selection for parsing and wMA data smoothing parameters for various data sets obtained from fatigue tests conducted at various G_{IIimax} loadings are listed in Table 4. For each of the fatigue data set, the graded parsing was carried out in such a way that the cycle selection was kept constant up to delamination onset and after onset the cycle selection was graded uniformly till the fracture. To clarify the parsing method, a brief cycle selection procedure for parsing is explained for IM7-2 specimen by using the parsing selection parameters from Table 4. The number of load cycles for damage onset for this specimen is 444 and is rounded to 450. Every n^{th} cycle selection for parsing is as follows: from 1 to 450 cycles select every 10^{th} cycle's cycle number and compliance; from 450 to 630 cycles select every 5^{th} cycle's cycle number and compliance; from 630 to 720 cycles select every 2^{nd} cycle's cycle number and compliance; and from 720 to 812 (fracture) cycles select every cycle's cycle number and compliance. Note from 450 cycles (onset) onwards, cycle selection number is decreasing (downward grading) till cycles for fracture. After graded parsing, wMA data smoothing with a moving average interval of 5 was applied on parsed compliance data using ΔN as MA weight.

Table 4
Data parsing and smoothing parameters.

Specimen #	G_{IIimax}/G_{IIc}	Cycles Range		Every N^{th} cycle selection (for parsing)	wMA[b] interval
		From	To		
IM7-1	0.6	1	210[a]	5	5
		210	270	2	
		270	333	1	
IM7-6		1	150[a]	5	
		150	177	2	
		177	207	1	
IM7-2	0.5	1	450[a]	10	5
		450	630	5	
		630	720	2	
		720	812	1	
IM7-7		1	510[a]	10	
		510	620	5	
		620	676	2	
		676	732	1	
IM7-3	0.4	1	1880[a]	20	5
		1880	2240	10	
		2240	2420	5	
		2420	2600	2	
		2600	2672	1	
IM7-8		1	1540[a]	20	
		1540	1920	10	
		1920	2110	5	
		2110	2300	2	
		2300	2351	1	
IM7-4	0.3	1	9700[a]	100	5
		9700	12,100	50	
		12,100	13,340	20	
		13,340	13,950	10	
		13,950	14,260	5	
		14,260	14,414	2	
		14,414	14,568	1	
IM7-9		1	12,700[a]	100	
		12,700	15,500	50	
		15,500	16,900	20	
		16,900	17,610	10	
		17,610	17,960	5	
		17,960	18,134	2	
		18,134	18,308	1	

[a] Cycles until onset for each specimen.
[b] Weighted MA interval is same for all specimens.

Fig. 9 shows an example of compliance vs. the number of loading cycles for the parsed and smoothed data set. The plot of C vs. N (parsed and smoothed) as shown in Fig. 9 is much better and smoother than the results in Fig. 6. The gradiently parsed and wMA smoothed compliance data was used to calculate the delamination length at each data point, using Eq. (9) along with the CC fit constants from Table 1. The calculated *a* values, cycle number and the load were used to generate the G_{IImax} and da/dN results for every specimen. During data reduction it was observed that some of the calculated da/dN values were negative and those values were set equal to a small value of 25.4e−09 mm/cycle. Then, weighted MA data smoothing with a moving average interval of 5 was applied on da/dN data using ΔN as MA weight. The plot of parsed/wMA smoothed fatigue crack growth rate, da/dN versus G_{IImax} is shown in Fig. 10. It is clearly seen in Fig. 8 that the raw fatigue crack growth rate is completely scattered and no clear distinction between the delamination onset and linear growth rate regions. On the other hand, the parsed and smoothed fatigue crack growth rate (see Fig. 10) clearly shows all three regions, namely, the delamination onset at relatively constant G_{IImax}, linear growth rate and fracture. The aforementioned graded parsing and wMA data smoothing technique was used for reducing fatigue data of all the specimens. The present parsing and weighted MA data smoothing method is simpler in comparison to the fatigue data reduction method used in [23,25,26] which is difficult and computationally intensive.

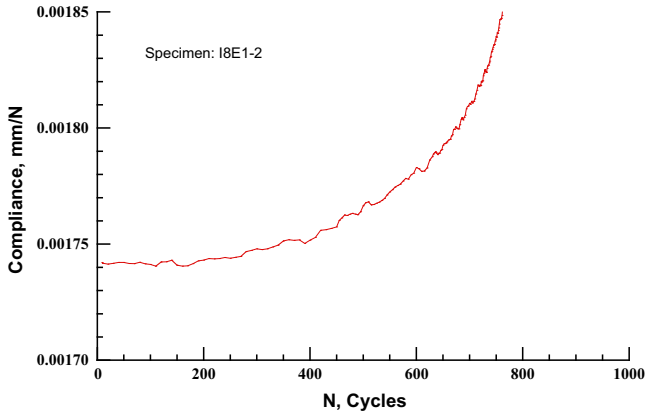

Fig. 9. Plot of compliance (parsed and smoothed) as a function of fatigue cycles.

6. Results and discussions

6.1. Fatigue delamination onset life and threshold energy release rate

The number of cycles corresponding to 1% increase of the specimen compliance was recorded for establishing the delamination onset life. Table 5 summarizes the onset lives for specimens tested

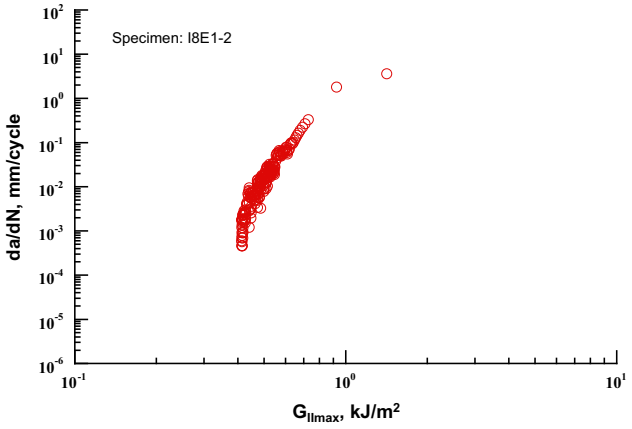

Fig. 10. Plot of delamination growth rate, da/dN (Parsed and smoothed) vs. G_{IIimax}.

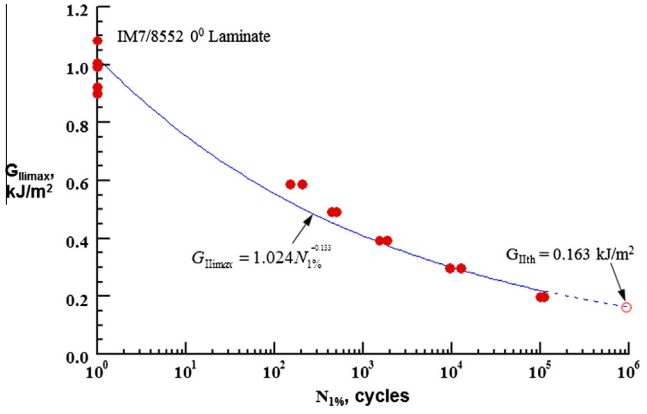

Fig. 11. Variation of fatigue onset life with G_{IIimax} for all specimens.

at various G_{IIimax} loadings. Fig. 11 shows a plot of G_{IIimax} versus $N_{1\%}$ for both sets of specimens. From the figure it is clear that the results of both the specimen sets are in agreement with each other for most of the data. A power law equation fit was performed for both data sets, including the average G_{IIc} value using the Kaleidagraph data plotting software to determine the G_{II} threshold (G_{IIth}) below which delamination should not occur (see Fig. 11). The equation was found to be

$$G_{IIimax} = DN_{1\%}^{n} \tag{12}$$

with constants D = 1.024 and n = −0.133. The threshold energy release rate (G_{IIth}) was calculated from Eq. (12) when N = 10^6 cycles and was found to be 0.163 kJ/m^2. This G_{IIth} was used to develop constants in delamination growth rate equation. The present G_{IIth} value differs from the Marunda's [31] reported value (G_{IIth} = 0.123 kJ/m^2 (0.7 lb-in/in^2)) for AS4/8552 composite laminate and also differs from G_{IIth} value (0.088 kJ/m^2 (0.5 lb-in/in^2)) calculated from delamination onset equation reported by O'Brien et al. [23] for IM7/8552 composite laminate. This difference in G_{IIth} value is perhaps because of the different type of initial crack configuration used, i.e. blunt Teflon insert (no-precracked) configuration in the present case versus sharp precracked configuration in O'Brien et al. and Marunda's study.

6.2. Fatigue delamination growth rate

Delamination growth rate (da/dN) versus G_{IImax} for all four test cases is plotted in log-log scale in Figs. 12–15. The two different symbols in the plots represent the test data from the two specimens. As previously stated, all test specimens were taken from the same panel. From the figures it is clear that the growth rate

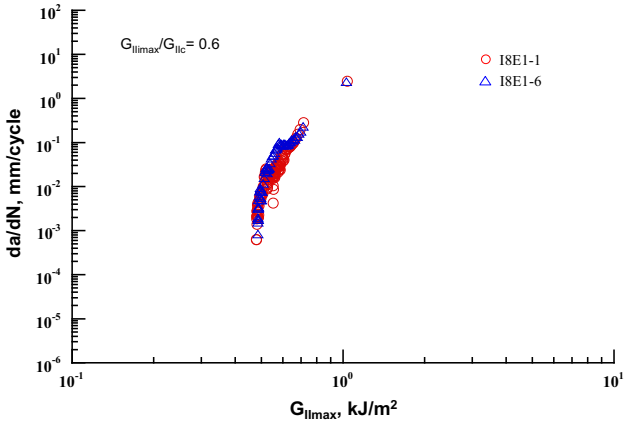

Fig. 12. Plot of delamination growth rate (da/dN) vs. G_{IImax} for G_{IIimax}/G_{IIc} = 0.6.

data sets of both the specimens overlap each other; thus indicating repeatability of the results and also indicating the good quality of the laminate and specimen preparation. An examination of data in Figs. 12–15 shows that there are three distinct regions: onset, linear growth, and final fracture where the G_{IImax} approaches G_{IIc}. The data in Figs. 14 and 15 shows a flattening near the fracture region because the delamination front approach the central load point, where the compliance equation parameters *A* and *m* become invalid and hence the calculated G_{IImax}. Taking this inaccuracy into consideration and G_{IImax} has to increase as the delamination front approach the load point, the flattening trend is ignored and da/dN is assumed to increase with G_{IImax}.

All eight specimens' delamination growth rate data is superposed into one log-log plot as shown Fig. 16. In the figure notice

Table 5
Cycles for delamination onset for all specimens.

Specimen #	G_{IIimax}/G_{IIc}	G_{IIimax}, kJ/m^2	1% Compliance, mm/N	Crack extension corresponding to 1% compliance, mm	Cycles for onset, $\Delta N_{1\%}$
IM7-1	0.6	0.59	1.806E−03	0.589	209
IM7-6		0.59	1.703E−03	0.613	151
IM7-2	0.5	0.49	1.759E−03	0.611	444
IM7-7		0.49	1.662E−03	0.604	503
IM7-3	0.4	0.39	1.773E−03	0.578	1875
IM7-8		0.39	1.670E−03	0.598	1536
IM7-4	0.3	0.29	1.796E−03	0.589	9654
IM7-9		0.29	1.697E−03	0.602	12,711
IM7-5	0.2	0.20	1.984E−03	0.677	100,553
IM7-10		0.20	1.752E−03	0.654	112,227

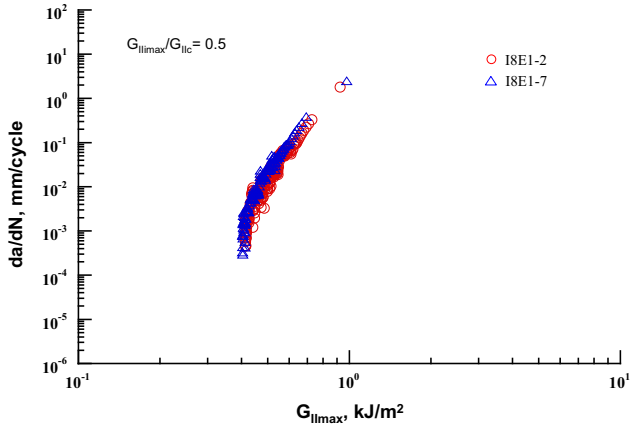

Fig. 13. Plot of delamination growth rate (da/dN) vs. G_{IImax} for G_{IIimax}/G_{IIc} = 0.5.

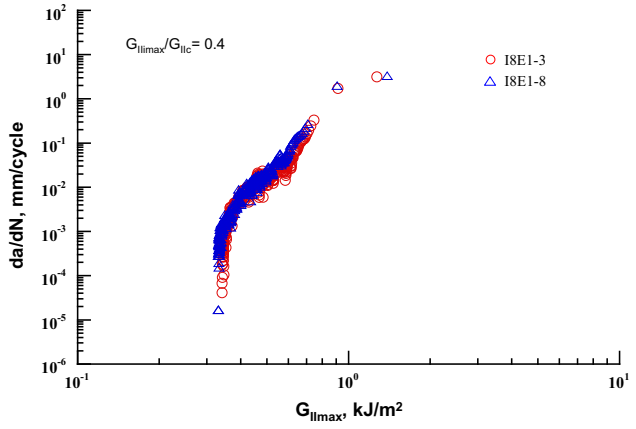

Fig. 14. Plot of delamination growth rate (da/dN) vs. G_{IImax} for G_{IIimax}/G_{IIc} = 0.4.

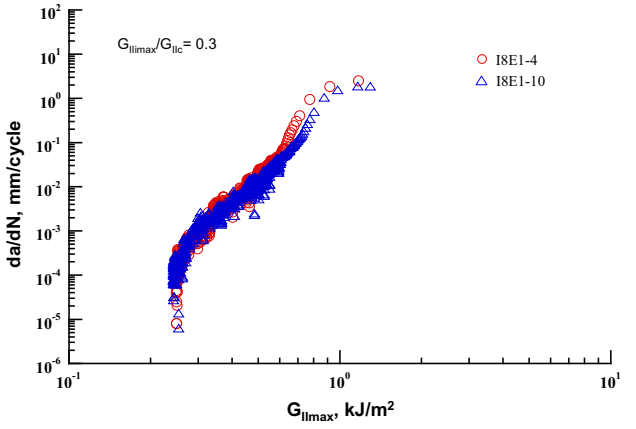

Fig. 15. Plot of delamination growth rate (da/dN) vs. G_{IImax} for G_{IIimax}/G_{IIc} = 0.3.

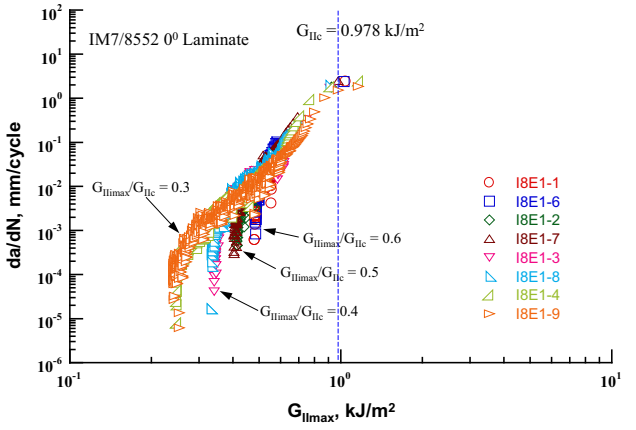

Fig. 16. Plot of delamination growth rate (da/dN) vs. G_{IImax} for all specimens.

the overlap except near the onset, this as expected will be a function of initial loading G_{IIimax}. The growth rate curves showed all three regions, namely delamination onset, linear growth rate, and unstable growth rate (fracture). In the delamination onset region, growth rate starts low initially and then increases at nearly constant G_{IImax} until it reaches a point where linear crack growth rate begins. In the linear growth rate region, the crack growth rate tends to increase linearly with increasing G_{IImax}. The behavior in onset and linear growth rate regions can be explained by considering how mode-II shear delamination initiate and propagate. The cycling from the Teflon insert requires the initial voids formation prior to the onset of delamination which slows down the initial crack growth rate. Then the shear delamination propagates through the coalescence of micro-tension cracks formed by the resolved shear stress ahead of the delamination front [32]. Once these voids start coalescing, the stable growth begins. Finally, in the unstable region the crack growth curves (see Fig. 16) at all G_{IIimax} load levels show fracture at approximately G_{IImax} = 0.98 kJ/m^2 (which is about the G_{IIc_NPC} of the material). It is clear from the Fig. 16 that the repeatability of da/dN data from specimen to specimen and the test starting at different G_{IIimax} are very well demonstrated unlike in other studies O'brien et al. [23] for mode-II, Murri [25] for mode-I, and Ratcliffe and Johnston [26] for mixed-mode. The studies in [23,25,26] focused on the onset and linear growth rate regions and seems like the authors truncated the crack growth rate data after linear region. One more important observation from Fig. 16 is that for IM7/8552 carbon/epoxy composite laminate, the maximum energy release rate (G_{IImax}) window between threshold and fracture is small when compared to metal's fatigue data. The G_{IImax} window between threshold and fracture is about 0.69 kJ/m^2 (difference between G_{IIimax} (0.290 kJ/m^2) and G_{IIc} (0.978 kJ/m^2)) and this value agrees closely with the fatigue growth rate data reported in [23,31]. The data in Fig. 16 also demonstrates that the single specimen test (G_{IIimax} = 0.3G_{IIc}) would be adequate to generate the complete growth rate results from onset to fracture.

The data in Fig. 16 was divided into three domains to develop a TFLM. They are:

1. Domain 1, is the part of the data from G_{IIth} to 1.3G_{IIimax}. Here only test data of G_{IIimax} = 0.3G_{IIc} is considered because this is the test which has low values of G_{IIimax}.
2. Domain 2, is the part of the data from 1.3G_{IIimax} to 0.7G_{IIc}. This is the region where the delamination growth rate follows the Paris law.
3. Domain 3, is the part of the data from 0.7G_{IIc} to fracture. Here, the specimen or the structure reaches static fracture when the delamination length under fatigue loading becomes large enough to cause fracture.

These three domains are used in developing TFLM for mode-II loading.

6.2.1. Development of total fatigue life model (TFLM)

A general equation in the form of Eq. (4) is chosen to develop a TFLM under mode-II stress state. In Eq. (4), α, β, D_1, and D_2 are the

material constants that are determined to meet the requirements of the three domains. The parameters α and β are determined from domain 2 data using Eq. (1). The constant D_2 is determined from the domain 3 ($0.7G_{IIc} \leqslant G_{IImax} \leqslant G_{IIc}$) test data using Eq. (3) from the known value of α and β using a trial and error approach. Finally, the constant D_1 is determined from the domain 1 test data using Eq. (2) from the known value of α and β.

6.2.2. Determination of TFLM constants

The linear region data from all the specimens were combined and plotted in the typical log-log form of a Paris law as shown in Fig. 17. A least square regression analysis in the form of Eq. (1) was performed on log(da/dN) versus log(G_{IImax}/G_{IIc}) data to determine the constants α and β. Based on the regression analysis, the constants were found to be α = 0.81 and β = 5.81. The Fig. 17 compares Eq. (1) with the test data. The delamination growth rates from experiments and from equation were in good agreement. The sensitivity of the α parameter was studied for α = 0.75, 0.80 and 0.85 with fixed value of β = 5.81. It was found that the α parameter was insensitive for the selected range. Similarly, sensitivity of the β parameter was studied for β = 5.7, 5.8 and 5.9 with fixed value of α = 0.8 and found that β parameter was also insensitive to small changes in its value. Fig. 18 compares the sensitivity of α and β with the test data. For the selected range of parameters α and β, Eq. (1) fits the test data very well. Therefore, α = 0.8 and β = 5.8 was chosen for developing TFLM. One more important observation from Fig. 17 is that the fatigue growth rate data sets of all the specimens nearly overlap each other which are an indication of repeatability of the test results and consistent quality of specimen's preparation. On the hand, the fatigue growth rate data sets reported in [23,31] were isolated from each other. Table 6 compares Paris law parameters (α and β) from the present study with O'Brien et al.'s [23] data and Marunda's [31] data for AS4/8552 laminate. The present α value (=0.8) differs from the α value ($\alpha = 6.84 \times 10^{-7}$, 9.00×10^{-7}, and 6.90×10^{-7}) reported in the literature by several orders of magnitude. This wide difference in α value is because of the different unit systems used for fatigue data reduction. The constant α depends on the units of the equation. The present results are based on SI unit system (da/dN in mm/cycle and G_{IImax} values in kJ/m^2) whereas O'Brien et al. and Marunda reported results in U.S. customary unit system (da/dN in in/cycle and G_{IImax} values in lb-in/in^2). On the other hand, the parameter β can be compared with the literature value because the β value must remain same irrespective of the unit system used. The present β value (=5.8) agrees well with β determined by O'Brien et al. and Marunda (5.45, 5.66, and 5.34).

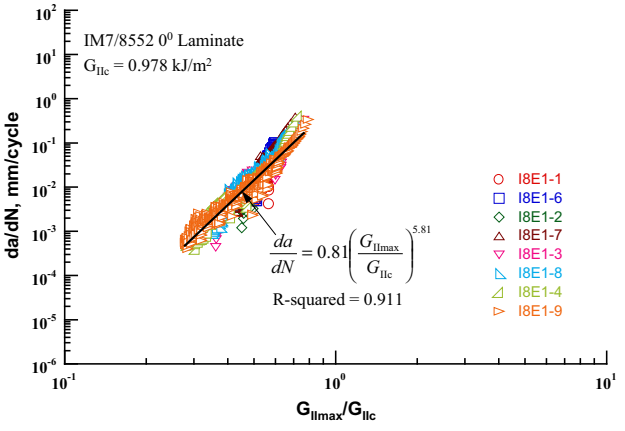

Fig. 17. Power law fit applied to the normalized delamination growth data for all specimens in domain 2.

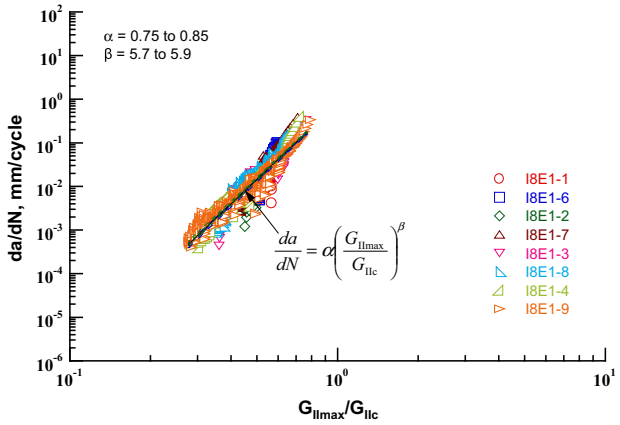

Fig. 18. Sensitivity of α and β parameters on predicted delamination growth rates in domain 2.

The exponent D_1 in Eq. (4) was determined by trial and error approach to best fit the data in domain 1 (G_{IIth} to $1.3G_{IIimax}$). The D_1 was found to be 12. A similar approach was used to determine D_2 in domain 3 ($0.7G_{IIc}$ to fracture) and D_2 was found to be 3. The sensitivity of the parameters D_1 and D_2 was studied by varying D_1 from 10 to 14 and D_2 from 2 to 4 and found that these parameters were insensitive for the selected range. The final equation of da/dN that covers all three domains is:

$$\frac{da}{dN} = 0.8\left(\frac{G_{IImax}}{G_{IIc}}\right)^{5.8} \frac{\left[1-\left(\frac{G_{IIth}}{G_{IImax}}\right)^{12}\right]}{\left[1-\left(\frac{G_{IImax}}{G_{IIc}}\right)^{3}\right]} \quad \text{valid for} \quad G_{IIth} \leq G_{IImax} \leq G_{IIc} \tag{13}$$

Fig. 19 compares the Eq. (13) with the test data. The delamination growth rates predicted from Eq. (13) and from experiments were in good agreement.

6.2.3. Fatigue delamination growth rate in terms of ΔG_{II}

The reliable total fatigue life model should reflect both the influence of the load ratio R and the fatigue behavior. Therefore, in order to account for the effect of cyclic loading ratio, R, the fatigue growth rate data is also reduced in terms of da/dN vs. ΔG_{II} because the range of energy release rate, ΔG_{II}, is a measure of the influence of loading ratio, R. The ΔG_{II} can be expressed in terms of R and G_{IImax} as follows.

The range of energy release rate, ΔG_{II}, is defined as

$$\Delta G_{II} = G_{IImax} - G_{IImin} \tag{14}$$

where G_{IImax} and G_{IImin} are the maximum and minimum values of the energy release rate corresponding to the maximum and minimum loads, respectively. From Eq. (6), it can be shown that

$$\frac{G_{IImin}}{G_{IImax}} = \frac{P_{min}^2}{P_{max}^2} = R^2 \qquad \because R = \frac{P_{min}}{P_{max}} \tag{15}$$

Alternatively,

$$\Delta G_{II} = (1 - R^2) G_{IImax} \tag{16}$$

In the present fatigue test, the load ratio R chosen was 0.1. Therefore, the ΔG_{II} becomes

$$\Delta G_{II} = 0.99 G_{IImax} \tag{17}$$

This means that all the plots shown in Figs. 12–16 shifts left by a factor R^2 (0.01) and the shape of the curve remain unchanged. In other words, R^2 acts like a shift factor for the fatigue delamination

Table 6
Comparison of Paris law parameters.

Authors	Material	Specimen type	$\frac{da}{dN}=\alpha\left(\frac{G_{IImax}}{G_{IIc}}\right)^{\beta}$	
			α	β
Present, SI unit	IM7/8552	NPC	8.10E−01	5.81
O'brien et al. [23]	IM7/8552 (Source 1)	PC	6.84E−07	5.45
O'brien et al. [23]	IM7/8552 (Source 2)	PC	9.00E−07	5.66
Marunda [31]	AS4/8552	PC	6.90E−07	5.34

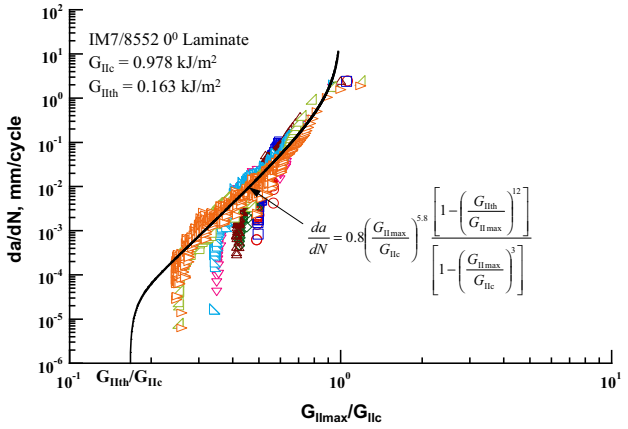

Fig. 19. Comparison of total fatigue life equation with the test data.

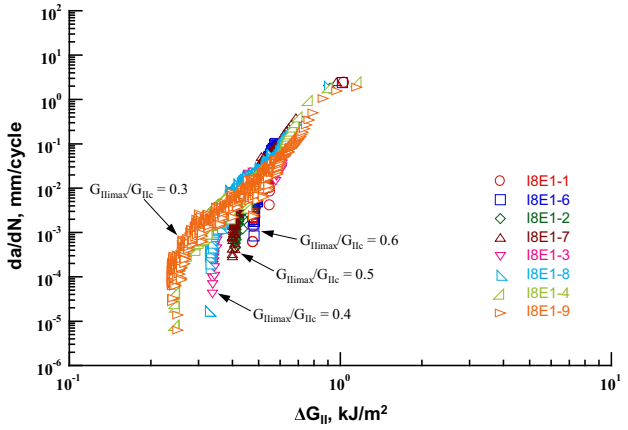

Fig. 20. Plot of delamination growth rate (da/dN) vs. ΔG_{II} for all specimens.

growth rate curves. Fig. 20 shows the resulting delamination growth rates expressed in terms of ΔG_{II} for all specimens at all four G_{IImax} loadings.

7. Conclusions

This paper presents a method of developing Total Fatigue Life Model (TFLM) for a unidirectional composite laminate with a delamination subjected to mode-II stress state. The model includes three domains of delamination growth rates, namely, the middle Paris domain (domain 2), and two end domains: onset and unstable fracture. The constants in the equation were determined from fatigue and fracture test data of End Notched Flexure (ENF) specimens for IM7/8552 carbon/epoxy composite laminate. The mode-II fracture toughness, G_{IIc} was determined from fracture tests and it was 0.978 kJ/m^2 for NPC specimens and 0.696 kJ/m^2 for PC specimens. The NPC fracture toughness (G_{IIc_NPC}) was used as the baseline. The fatigue crack growth rate data was generated by load controlled constant amplitude cyclic load fatigue tests at initial G_{IIimax} values of 60, 50, 40, and 30% G_{IIc}. The stress ratio (R) used was 0.1. The fatigue onset life was determined by 1% compliance change for different G_{IIimax} value. This data was extrapolated using the power law for one million cycles (N) to determine the threshold energy release rate, G_{IIth} which is $0.167G_{IIc}$. A graded parsing followed by weighted Moving Average method was used for fatigue data smoothing. The secant method was used to calculate the delamination growth rate, da/dN vs. G_{IImax} for each fatigue specimen. The fatigue test results were used to develop the total fatigue life model in the form of $\frac{da}{dN}=\alpha\left(\frac{G_{IImax}}{G_{IIc}}\right)^{\beta}\left[1-\left(\frac{G_{IIth}}{G_{IImax}}\right)^{D_1}\right]\Big/\left[1-\left(\frac{G_{IImax}}{G_{IIc}}\right)^{D_2}\right]$ where α, β, D_1, and D_2 are the material constants. These parameters for IM7/8552 carbon/epoxy composite laminates are 0.81, 5.81, 12 and 3, respectively. The developed delamination growth rate model fits the fatigue test data very well in all three domains. The Paris law exponent (β) agreed very well with the values reported in the literature. The effect of R on the da/dN vs. G_{IImax} curve is to cause horizontal shift of the data by R^2. In addition, the test data also demonstrated that a single fatigue test at $G_{IIimax} = 0.3G_{IIc}$, would be sufficient to generate the complete da/dN growth rate data instead of multiple tests using different values of G_{IIimax}.

Acknowledgments

The authors acknowledge the support of NRTC through grant # W911W6-11-2-0012 and NASA URC-Center for Aviation Safety (grant # NNX09AVO8A). Authors thank Mr. Matthew Sharpe for help in fabricating the IM7/8552 laminates and preparation of specimens and Mr. John Skujins for help in carrying out fatigue tests.

References

[1] Pipes R Byron, Pagano NJ. Interlaminar stresses in composite laminates under uniform axial extension. J Compos Mater 1970;4(4):538–48.
[2] O'Brien TK. Characterization of delamination onset and growth in a composite laminate. In: Reifsnider KL, editor. Damage in Composite Materials, ASTM STP 775. Philadelphia: American Society for Testing and Materials; 1982. p. 140–67.
[3] Pagano NJ. Interlaminar response of composite materials, composite materials series, vol. 5. Amsterdam: Elsevier; 1989.
[4] Salpekar SA, O'Brien TK, Shivakumar KN. Analysis of local delaminations caused by angle ply matrix cracks. J Compos Mater 1996;30(4):418–40.
[5] Priddle EK, Marshall P. Fatigue design consideration of small surface defects of AISI type 316 stainless steel. I Mech E Conference Publications, vol. 2. I Mech E; 1986. p. 533–46.
[6] Shivakumar K, Chen H, Abali F, Le D, Davies C. A total fatigue life model for Mode I delaminated composite laminates. Int J Fatigue 2006;28(1):33–42.
[7] Shivakumar K, Chen H, Abali F. Mode I delamination growth rate model for glass/vinyl ester composites. In: Proceedings of 18th Annual Technical Conference of ASC, Gainesville, Florida, 22, October 19–22.
[8] Shivakumar K, Chen H, Abali F. Total fatigue life modeling for composite laminates under Mode I loading. In: Gibson Ronald F, editor. American society for composites series on advances in composite materials volume 3: fatigue of composite materials. DEStech Publications; 2012.
[9] Chen H, Shivakumar K, Abali F. A comparison of total fatigue life models for composite laminates. Fatigue Fract Eng Mater Struct 2006;29:31–9.

[10] Poursartip A. Characterization of edge delamination growth in laminates under fatigue loading. In: Johnston Norman J, editor. Toughened composites, ASTM STP 937. Philadelphia: American Society for Testing and Materials; 1987. p. 222–41.
[11] Abali F, Shivakumar K, Chen H. Delamination growth rate equation for T800H/3900-2 composite laminate, AIAA-2004-1927, p. 4371.
[12] Chen H, Shivakumar K, Abali F. Application of total fatigue life model to T700 carbon/vinyl ester composite. Composites: Part B 2008;39:36–41.
[13] Bathias C, Laksimi A. Delamination threshold and loading effect in fiber glass epoxy composite. In: Johnson WS, editor. Delamination and debonding of materials, ASTM STP 876. Philadelphia: American Society for Testing and Materials; 1985. p. 217–37.
[14] Gustafson C, Hojo M. Delamination fatigue crack growth in unidirectional graphite/epoxy laminates. J Reinforced Plast Compos 1987;6:36–52.
[15] Mall S, Johnson WS, Everett Jr RA. Cyclic debonding of adhesively bonded composites. In: Mittal KL, editor. Adhesive joints: their formation, characteristics, and testing. New York: Plenum Press; 1984. p. 639–58.
[16] Mall S, Johnson WS. Characterization of mode I and mixed-mode failure of adhesive bonds between composite adherents. In: Whitney JM, editor. Composite materials: testing and design (seventh conference). ASTM STP 893. Philadelphia: American Society for Testing Materials; 1986. p. 322–34.
[17] O'Brien TK. Towards a damage tolerance philosophy for composite materials and structures, vol. 1059. ASTM Special Technical Publication; 1990. p. 7.
[18] Kardomateas GA, Pelegri AA, Malik B. Growth of internal delaminations under cyclic compression in composite plates. J Mech Phys Solids 1995;43(6):47–68.
[19] Hojo M, Matsuda S, Tanaka M, Ochiai S, Murakami A. Mode I delamination fatigue properties of interlayer-toughened CF/epoxy laminates. Compos Sci Technol 2006;66:665–75.
[20] Hojo M, Ando T, Tanaka M, Adachi T, Ochiai S, Endo Y. Modes I and II interlaminar fracture toughness and fatigue delamination of CF/epoxy laminates with self-same epoxy interleaf. Int J Fatigue 2006;28:1154–65.
[21] Hojo M et al. Mode I fatigue delamination of Zanchor-reinforced CF/epoxy laminates. Int J Fatigue 2010;32:37–45.
[22] Shivakumar K, Shivalingappa L, Chen Huanchun, Akangah Paul, Swaminathan Gowthaman, Russell Jr Larry. Polymer nanofabric interleaved composite laminates. AIAA J 2009;47(7):1723–9.
[23] O'Brien TK, Johnston WM, Toland GJ. Mode II interlaminar fracture toughness and fatigue characterization of a graphite epoxy composite material, National Aeronautics and Space Administration Technical Memorandum NASA/TM-2010-216838; 2010.
[24] Argüelles A, Viña J, Fernández-Canteli A, Viñaa I, Bonhomme J. Influence of the matrix constituent on mode I and mode II delamination toughness in fiber-reinforced polymer composites under cyclic fatigue. Mech Mater 2011;43:62–7.
[25] Murri GB. Evaluation of delamination onset and growth characterization methods under mode I fatigue loading, National Aeronautics and Space Administration Technical Memorandum NASA/TM-2013-0010557; 2013.
[26] Ratcliffe JG, Johnston Jr WM. Influence of mixed Mode I–Mode II loading on fatigue delamination growth characteristics of a graphite epoxy tape laminate. In: Proceedings of the ASC 29th technical conference, La Jolla, California, U.S.A., 8–10 September.
[27] ASTM E 647–00. Standard test method for measurement of fatigue crack growth rates. Annual Book of ASTM Standards, vol. 03.01. ASTM International; 2014.
[28] ASTM Standard D7905/D7905M-14. Standard test method for determination of the Mode II interlaminar fracture toughness of unidirectional fiber-reinforced polymer matrix composites. West Conshohocken, PA: ASTM International; 2014.
[29] Shivakumar K, Panduranga R, Skujins J, Miller S. Assessment of Mode-II fracture tests for unidirectional fiber reinforced composite laminates. J Reinforced Plast Compos 2015;34(23):1905–25.
[30] ASTM Standard D6115–97. Standard test method for Mode I fatigue delamination growth onset of unidirectional fiber-reinforced polymer matrix composites. West Conshohocken, PA: ASTM International; 2011.
[31] Marunda Torrence S. Fatigue life modeling of AS4/8552 carbon/epoxy composite laminate under Mode II stress state (M. S Thesis). North Carolina A&T State University; 2015.
[32] O'Brien TK. Composite interlaminar shear fracture toughness: GIIc: shear measurement or sheer myth? Composite materials: fatigue and fracture, Seventh Volume, ASTM STP 1330; 1998; p. 3–18.